Recent Star Formation in Local Group Galaxies from HST Imaging

Luciana Bianchi, Alin Tolea, Boryana V. Efremova

Center for Astrophysical Sciences, Dept. of Phys. & Astr., The Johns Hopkins University

Abstract

We present results from an on-going study of stellar populations in the Local Group galaxies M33 and NGC6822 from multi-band imaging obtained with several HST programs. The HST photometry provides a detailed characterization of the resolved stellar populations. The stellar physical parameters are derived by comparing the observed colors to model colors. We show two different methods and sample results. Our on-going programs include similar studies in the LMC and M31.

This study of the resolved stellar population is complemented by UV surveys of nearby galaxies in their entirety, performed with GALEX in two Ultraviolet bands, and with a variety of corollary data in the optical and IR (see posters by Bianchi et al. "Recent Star Formation in Local Group Galaxies from the GALEX surveys", and by Thilker, Bianchi et al.)

Introduction

Local Group galaxies represent an ideal laboratory for resolved studies of stellar populations with HST and VLT, and span a large range of metallicity and galaxy types, providing important clues to the factors regulating star formation. The results for these benchmark populations are the key to interpret integrated properties of distant galaxies, to ultimately reconstruct the history of star formation in the universe.

With several HST programs since cycle 1, we have been studing stellar population in selected fields across Local Group galaxies. Here we show examples of results from several recent programs, covering areas across the galaxies M33 and NGC6822.

Data and method

We observed a large number of fields across the galaxies M33, NGC6822, M31 and LMC, using the HST WFPC2 and ACS cameras, with a number of programs from cycle 1 todate. We use a variety of filters, including U,B,V and two UV filters (F170W and F255W), because the availability of several independent colors allows us to derive more than one parameter consistently: $T_{\rm eff}$, extinction, and in some cases also the type of extinction (characterized by the value of R_V).

The intrinsic SEDs of stellar objects depend mainly on the stellar temperature $T_{\rm eff}$, (to a much smaller extent on gravity and metallicity). The selective interstellar extinction (reddening) modifies the intrinsic SED, to an extent proprtional to E(B-V), and with a wavelength dependence varying according to the dust properties along the line of sight. Therefore, we constructed a vast grid of stellar models (Bianchi & Garcia 2004), reddened them with various amounts and types of extinction, and applied the transmission curves of the photometric filters to obtain a grid of model magnitudes. Comparison of the observed and model SED allows us in principle to derive both $T_{\rm eff}$ and E(B-V), provided enough colors are measured.

To compare the photometric SED to model SEDs, we proceed in two ways. First, we can construct "reddening-free" indices, "Q", by combining three or more bands (two or more colors), and assuming a certain type of reddening. For example, using three bands i, j, k we can construct the index:

$$Q_{(i,j,k)} = (Mag_i - Mag_j) - C_{(i,j,k)} \times (Mag_j - Mag_k) \quad (1)$$

$$C_{(i,j,k)} = E_{(Mag_i - Mag_j)}/E_{(Mag_j - Mag_k)} \quad (2)$$

The well known two problems are: (1) that each "reddening-free" index is actually "reddening-free" only within a limited parameter range, (2) the index can be multi-valued in certain parameter ranges. Therefore, one must be careful to only use a given index "Q" in the range of observed colors where it is a linear, unique function of $T_{\rm eff}$, and where it is reddening-$''free''$ to an acceptable extent. Both problems, pointed out by several authors empirically in the past (e.g. Massey et al. 1995, Bianchi et al. 2001, Romaniello et al. 2002, Maíz 2004), are illustrated in a quantitative way in the figure below, where "Q" indices are constructed from our grid of model magnitudes, for a range of extinction types and stellar parameters.

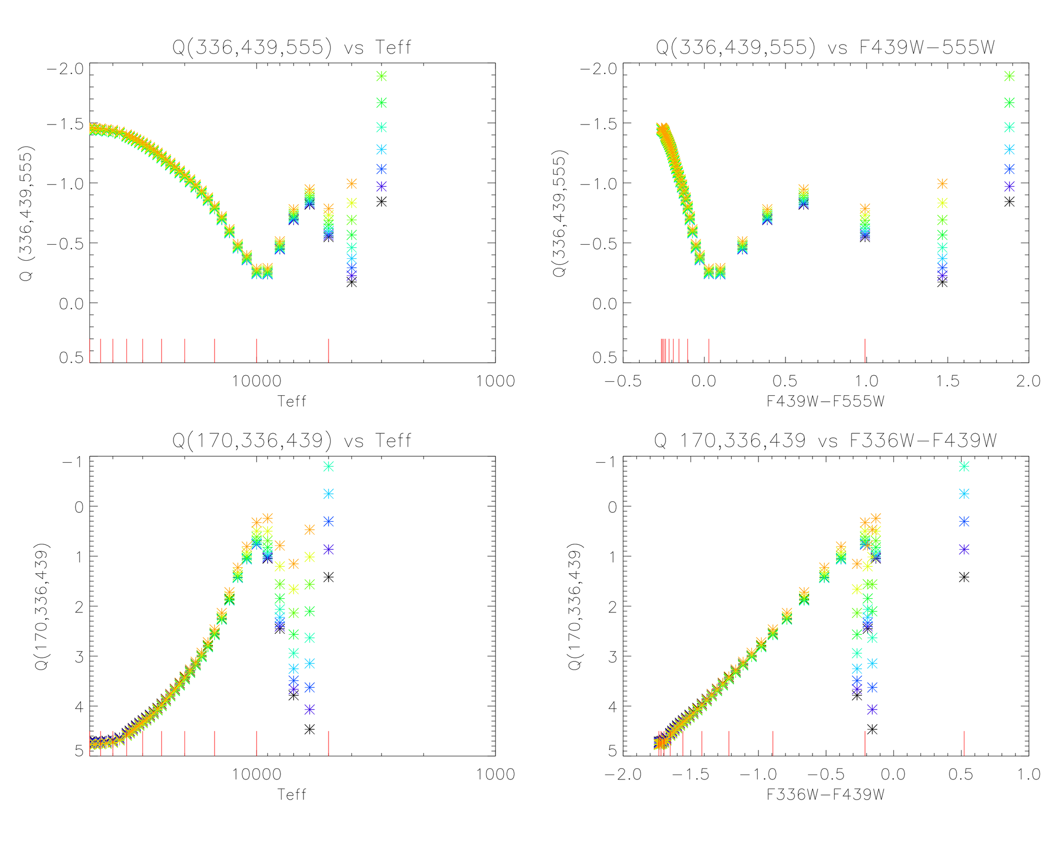

Figure 1. Two reddening-free indices, constructed from our grid of model magnitudes, are shown as a function of $T_{\rm eff}$ and as a function of color. Top panels: the traditional $Q(U,B,V)$ index, bottom panels: $Q(far-UV,U,B)$. The different colors indicate steps of 0.1 in E(B-V), starting from 0. (black). The red ticks are for 5000 K intervals of $T_{\rm eff}$, starting at 5000 K. From these plots, one can appreciate the range where the index is actually "reddening-free".

Preprints, reprints, info at http://dolomiti.pha.jhu.edu

In the second method, we find the best model SED fit to the observed magnitudes, weighted by their corresponding photometric errors, deriving - as free parameters - $T_{\rm eff}$ and E(B-V) [and sometimes reddning type]. While this method has the advantage of using all bands at once, the limitation remains of possible multiple solutions in some cases, and must be taken into account. Examples (using Maíz (2004) fitting method "CHORIZOS") are shown in Figure 7.

In either case, using "Q"-indices or fitting the photometric SEDs, for objects which have a unique solution and where either method is valid we determine all parameters concurrently, while for the other objects we interpolate the value from E(B-V) from nearby objects with independent extinction determinations, and derive $T_{\rm eff}$. A more detailed description can be found in our papers.

HST Imaging in M33

With Bianchi's HST programs GO 6038, 8207, 9127 and 9828, we covered 27 WFPC2 fields sampling intersting regions across the nearby spiral galaxy M33. We used several filters, in most cases including U, B, V (F336W, F439W and F555W) as well as two UV filters (F170W and F255W), for better sensitivity to hot massive stars (young populations) and extinction. Figure 2 below shows the location of the fields.

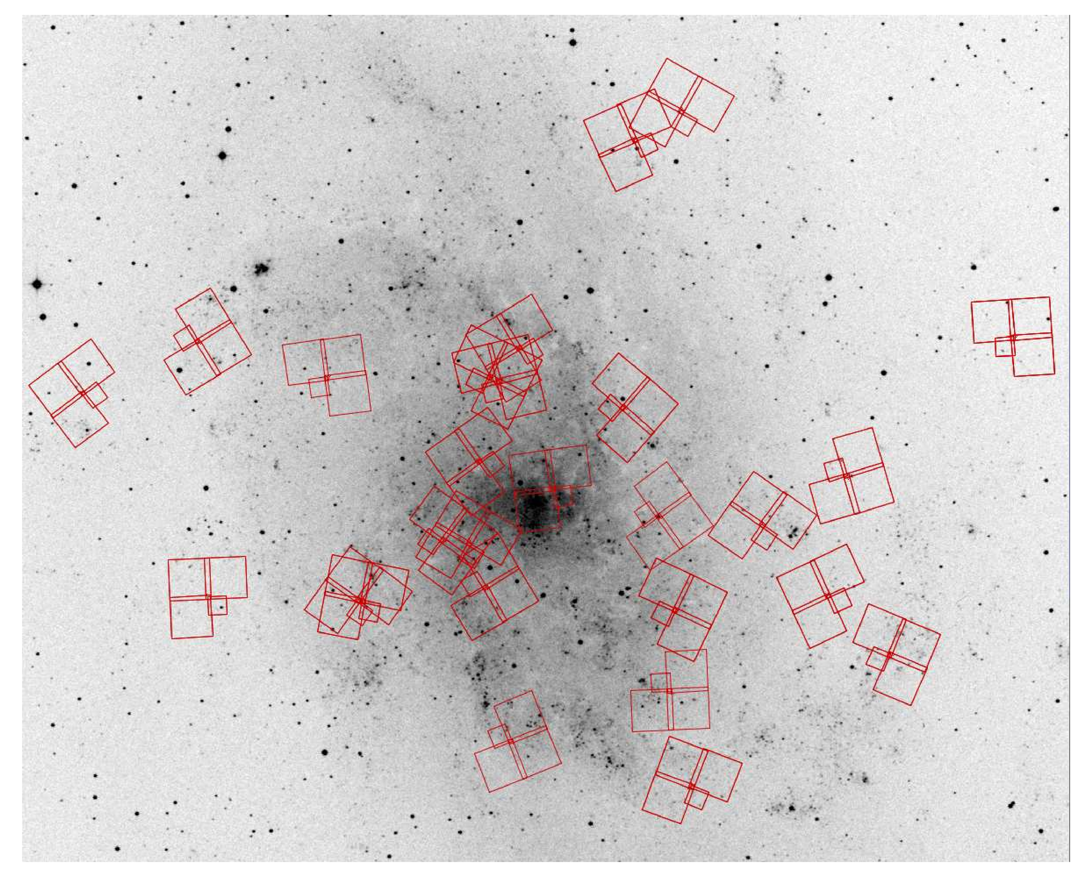

Figure 2. Ground Based Digitized Sky Survey Image of M33 with the location of 27 HST WFPC2 fields from HST programs GO6038, 8207, 9127 and 9828 superposed. The field is approximately 50 by 40 arcmin.

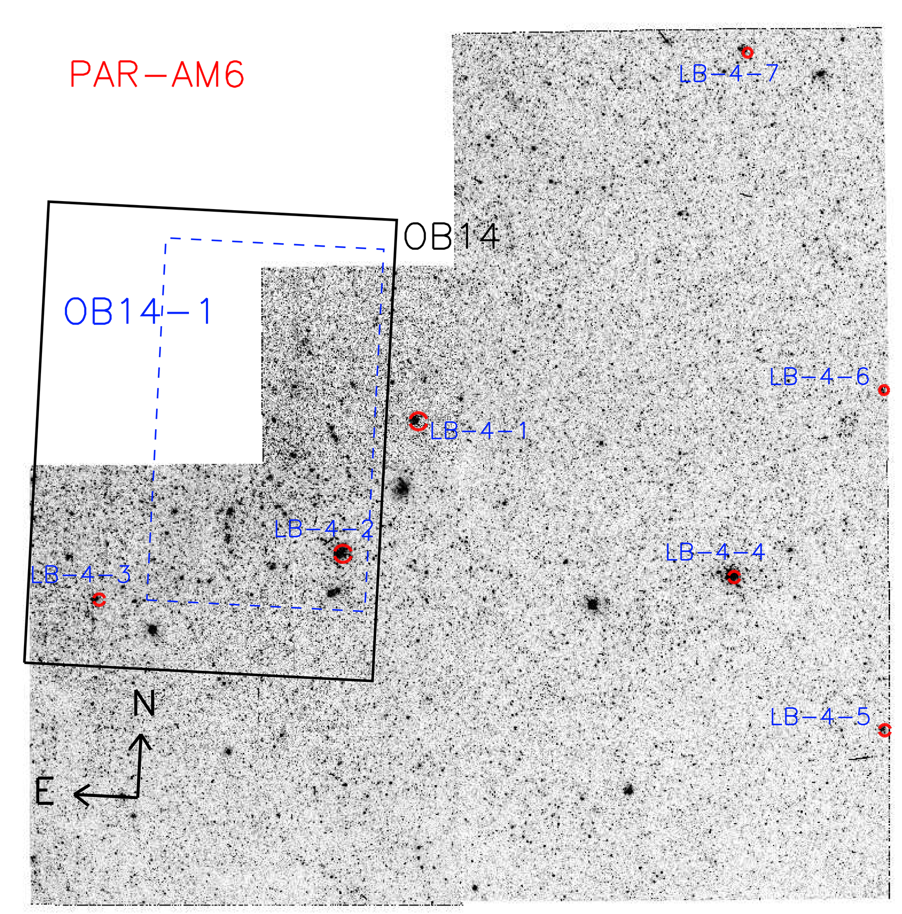

Figure 3. F555W mosaic of a sample field in M33. An OB association from Humphreys and Sandage (1980) is outlined and labeled in black. Our identified young populations are outlined in blue. Stellar clusters from Chandar Bianchi and Ford (1999, 2001) are labeled in blue.

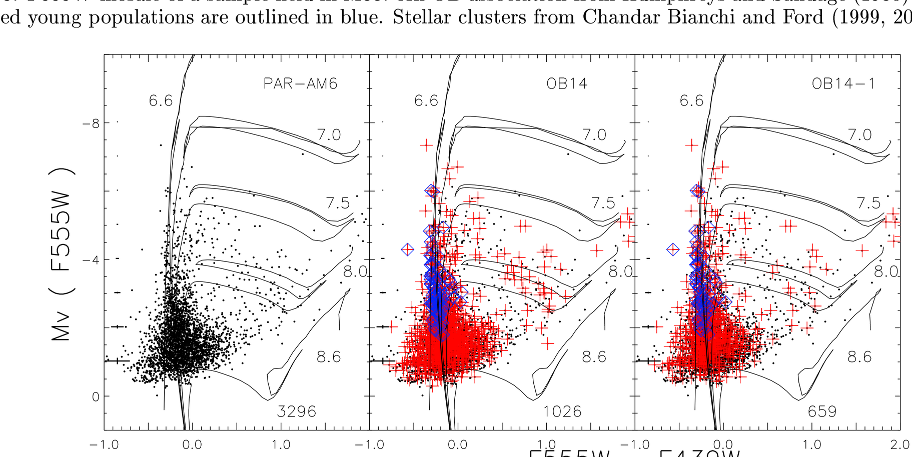

Figure 4. HR diagrams for the field shown above. Isochrones with Z=0.008 from Girardi et al. (2002), are superimposed and labeled with ages [log years]. The first panel is for the entire field. Black points are all the stars in the field, red and blue symbols are the stars within the boundaries of each OB association

HST Imaging in NGC6822

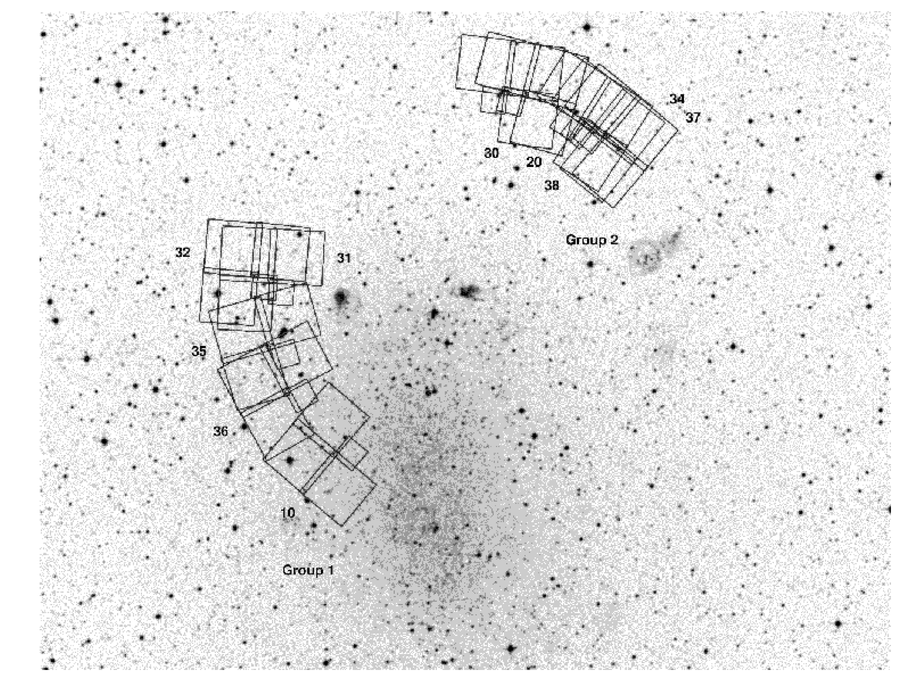

Figure 5. In NGC6822, 11 fields were imaged with WFPC2 as part of Bianchi's program HST GO8675. Deep exposures were taken with five filters from far-UV to V (F170W, F255W, F336W, F439W, F555W) for a total of 110 images. Here the field locations are shown. None of these fields covers richest HII regions such as those observed and analysed by Bianchi et al. (2001). These data sample mainly the general field, and outer galaxy regions, thus complementing our previous program by exploring different environments in this galaxy. However, young massive stars are found in some of the fields (see figures below).

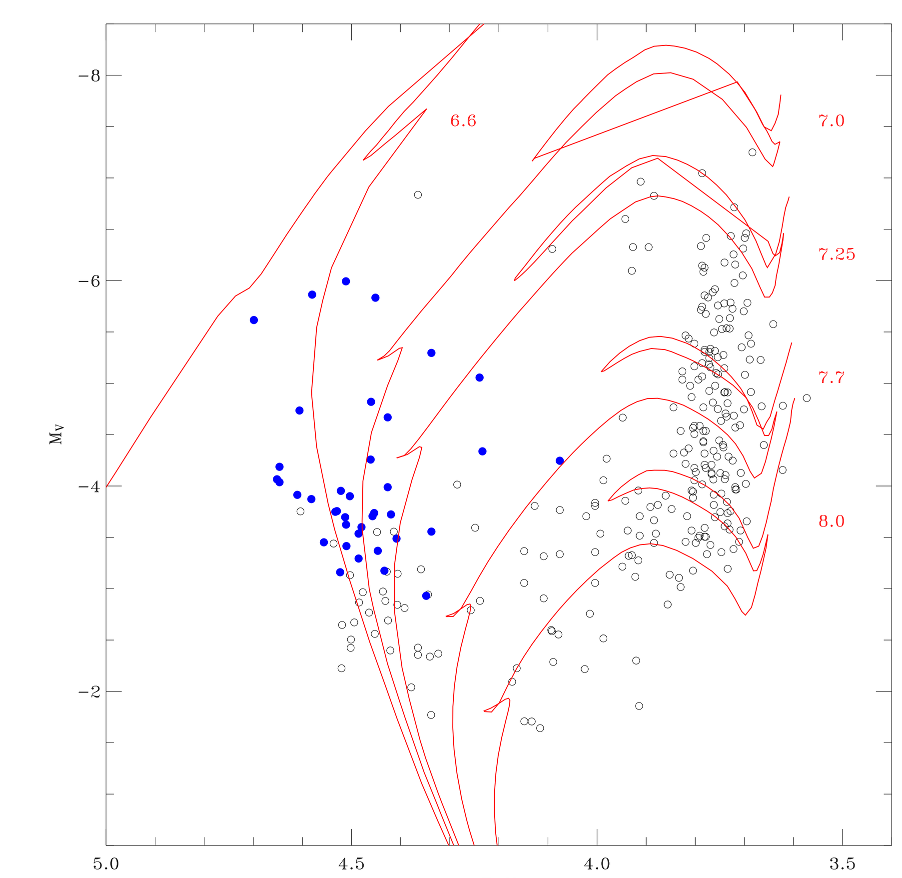

Figure 6. HR Diagram for the fields in NGC6822 shown in the above figure. In blue are the objects with good photometry in all filters: F170W, F255W, and U B V. Black points are objects with measurements in fewer filters (usually the far-UV band is missing). Superimposed (red lines) are isochrones from Padua models (Girardi et al. 2002) with log ages (yrs) indicated. $T_{\rm eff}$ and extinction were determined from the reddening-free indices, constructed using all available bands from our grid of stellar models, and restricting to the ranges where each index is linear, reddening-free and unique. A second method used to determine $T_{\rm eff}$ and extinction consists in fitting all the observed colors with model colors (examples in figure 7).

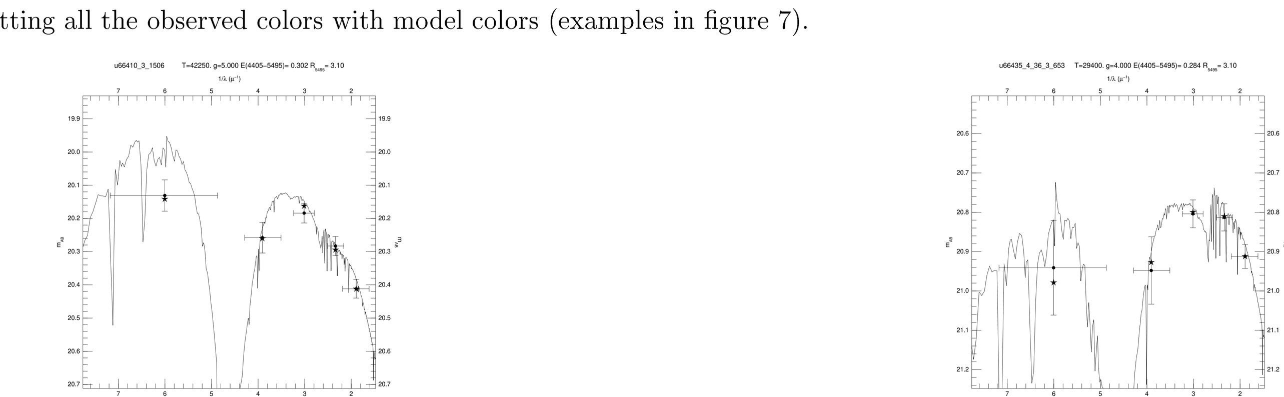

Figure 7. Examples of SED fits. Measured magnitudes are shown with their error (vertical bar), the width of the horizontal bar represents the band width of the filter. Both model magnitudes and the full resolution model spectrum are also shown. The fits were obtained using Maíz (2004)'s code CHORIZOS.

REFERENCES:

Bianchi, L., & Garcia, M., 2004, in preparation
Bianchi, L., Scuderi, S., Massey, P., & Romaniello, M. 2001, AJ, 121, 2020
Chandar, R., Bianchi, L. & Ford, H. C. 1999, ApJ, 517, 668
Chandar, R., Bianchi, L. & Ford, H. C. 2001, A&A, 366, 498
Girardi, L., Bertelli, G., Bressan, A., Chiosi, C. , Groenewegen, M.A.T., Marigo, P., Salasnich, B. & Weiss, A. 2002, A&A, 391, 195
Humphrreys, R. M & Sandage, A. 1980, ApJS, 44, 319
Maíz-Appellaniz, J., 2004, PASP, 116, 859
Massey, P., Armandroff, T. E., Pyke, R., Patel, K., & Wilson, C. D. 1995, AJ, 110, 2715
Romaniello, M. Panagia, N., Scuderi, S., Kirshner, R, 2002, AJ, 123, 915

This work was supported by NASA grants HST-GO-8675, HST-GO-9127 and NAG5-9219